

Accelerated dynamics simulations of interstitial-cluster growth

Stefan Birner,^{1,2} Jeongnim Kim,¹ David A. Richie,¹ John W. Wilkins,¹ Arthur F. Voter,³ and Thomas Lenosky⁴

¹*Department of Physics, Ohio State University, Columbus, OH 43210*

²*Walter Schottky Institute, TU Munich, D-85748, Garching, Germany*

³*Theoretical Division, Los Alamos National Laboratory, Los Alamos, NM 87545*

⁴*Finisar Corporation, Sunnyvale, CA 94089*

We apply parallel replica dynamics to simulate the growth of silicon interstitial clusters. Existing interstitial clusters are efficient traps for mobile interstitial and di-interstitial defects. For clusters involving more than four interstitials, many metastable structures are achieved by local bonding rearrangements. The shape of interstitial nuclei critically determines the final interstitial clusters. Once an elongated cluster is formed, additional captured interstitials diffuse in the chain direction and eventually settle at the chain ends, resulting in further elongation.

PACS numbers: 61.72.-y, 61.72.Cc, 61.72.Ji, 71.55.-i

Interstitial defects control the dopant diffusion in ion-implanted silicon by providing traps for and sources of mobile interstitials.¹⁻³ Understanding energetic and dynamical properties of interstitial defects is an essential step in accurately modeling the time evolution of dopant profiles.^{3,4} Recent theoretical studies of interstitial defects⁵⁻⁹ elucidate their growth path: interstitial clusters become more stable by adding more interstitials. This is consistent with the thermal behavior of boron transient enhanced diffusion with or without large-scale interstitial defects.^{1,2} However, the microscopic understanding of the critical steps leading to the cluster growth is limited. Cost for atomistic simulations grows prohibitively for the increasing complexity of the system. Furthermore, the long time scale involved with the diffusion and nucleation is not easily achieved by conventional molecular simulations involving many degrees of freedom.

The parallel-replica method¹⁰ extends the time scale of infrequent events by running a number of replicas, independent trajectories, in parallel. When the system makes a transition from one basin to another on any of the processors, the corrected time at which the transition occurred is simply the sum of times accumulated on all the processors up to that instant. All the trajectories are then restarted in the new basin, randomized independently for a dephasing period, and the procedure is repeated. This can be shown to give the exact classical evolution of system, in the sense that the state-to-state transitions, and the times at which they occur, are indistinguishable from a long trajectory on a single processor. Independently of atomistic potentials, parallel-replica simulations give gains in simulation time per wall-clock time nearly proportional to the number of replicas, provided the average time between transitions is long compared to the dephasing time.

Here we apply the parallel-replica (PR) method¹⁰ to study the growth of silicon interstitial clusters. The silicon-silicon interaction is described using a recently fit classical potential¹¹ of the modified embedded atom method (MEAM) form.¹² This MEAM potential has been extensively tested against *ab initio* calculations, particularly for defects in bulk silicon. We model the

cluster growth by (i) coalescence of randomly-distributed interstitials for small clusters and (ii) mobile-interstitial capture by an n -interstitial cluster. Local minimum configurations and transition states extracted from collected trajectories of many PR runs provide microscopic models for the interstitial-diffusion and interstitial-trapping processes. Using between 4 and 128 processors (dephasing time 1-2 psec), we achieved simulation times as long as 0.1 μ sec, allowing accurate estimations of dynamical quantities such as diffusion constants of mobile interstitial defects. Because we also used high temperatures to speed up the processes, the parallel efficiency ranged from low to nearly perfect depending on the case.

Small interstitial clusters: $n=2-4$. Randomly distributed isolated interstitials coalesce into small clusters. For example, di-interstitial I_2 clusters are invariably formed when two interstitials are located within the third-nearest-neighbor sites. At 500 and 800 K, four interstitials in a 512-atom unit cell form compact clusters, after making several interstitial jumps. Both constant-temperature MD and PR simulations give the activation energy barrier of $E_m=0.2$ eV for an interstitial jump. The diffusion constant for an interstitial I_1 is estimated as $D_I = D_I^0 e^{-E_m/k_B T}$ where $D_I^0 = 4.5 \times 10^{-6}$ cm²sec⁻¹.

Simulations with the classical MEAM potential give reliable information for small clusters. Specifically, I_2 clusters are as mobile as I_1 's with a migration activation energy of 0.1 eV. This is consistent with the *ab initio* and tight-binding predictions that I_2 's are important mobile components in interstitial-supersaturated silicon.⁶ The formation of a tri-interstitial cluster I_3 occurs in two steps: (1) formation of I_2 and (2) its subsequent capture of an interstitial. Among the local minimum structures identified is the compact I_3 with T_d symmetry.^{7,9}

Metastable precursors dominate the formation of an I_4 cluster. Figure 1 shows the local minima found during a PR run at 800 K of the I_4 formation. Within 0.2 nsec, a metastable I_4 cluster is formed, releasing 5.6 eV. Once a metastable I_4 cluster is formed, transitions between related structures and diffusion of the cluster occur for 2 nsec. After about 300 transitions, the cluster falls into the ground configuration (D_{2d} symmetry)

whose core structure is shown in Fig. 1. About 1 eV is released when the ground-state I_4 is formed by bonding rearrangements from metastable precursors. Both I_2 and I_3 clusters are precursors of an I_4 cluster, consistent with interstitial cluster growth models of small clusters.^{3,4}

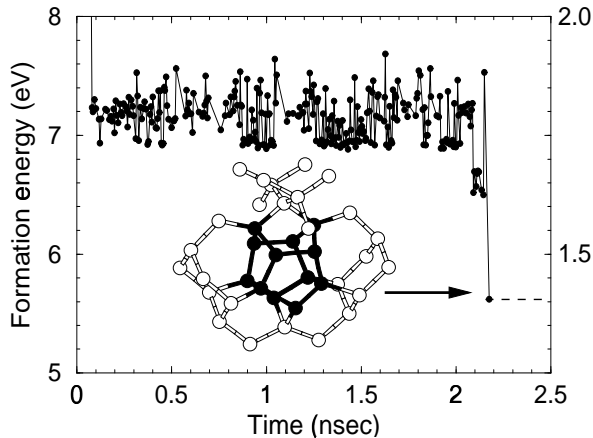


FIG. 1. Formation energy of a four-interstitial defect during a parallel-replica run at 800 K and the core structure of the ground I_4 - D_{2d} cluster. The starting configuration consists of four randomly distributed T-interstitials in a 512-atom cell. After 20 interstitial jumps, a metastable I_4 precursor is formed, releasing 5.4 eV (off the scale). Once the transition to I_4 - D_{2d} occurs, no more transitions are observed within 10 nsec.

The classically simulated I_4 ground state is in good agreement structurally and energetically with *ab initio* calculations^{7,8}: a low 1.4 eV formation energy versus 1.5 eV *ab initio* result. Both experiment³ and calculations^{5,7,8} predicted the I_4 - D_{2d} to be extremely stable. Indeed tens of nanoseconds additional simulation at both 500 and 800 K find no lower state.

Intermediate interstitial clusters: $n=5-20$. For the simulations of interstitial-cluster growth larger than $n=4$, we use a different approach. Starting configurations combine (i) an interstitial cluster I_n with (ii) an I_1 or I_2 placed at a distance far from the existing cluster. The final cluster I_{n+1} or I_{n+2} is then used as the initial cluster for subsequent simulations. These initial configurations are chosen to realize the assumption used in kinetic Monte Carlo simulations^{3,4}: a mobile interstitial defect is captured by a pre-existing immobile-interstitial cluster such as I_4 .

Our results can be summarized: with an existing interstitial cluster providing a capture nucleus, the cluster growth occurs by (i) interstitial capture at the cluster boundaries and (ii) subsequent local rearrangements of the core atoms to lower-energy structures.

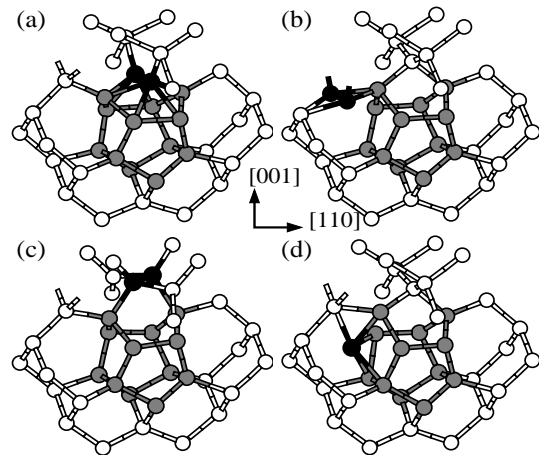


FIG. 2. Core structures of I_5 local minima identified by parallel-replica runs. The captured interstitial is shown as \bullet . Note that (a)-(c) contain split interstitialcy. Within MEAM, (a) is the ground structure. Metastable structures (b)-(d) are typically found at the moment of interstitial capture. Gray atoms denote the I_4 - D_{2d} structure that remains intact after formation of I_5 by an interstitial capture.

Consider the starting configuration of a compact I_4 cluster and an isolated interstitial. After several interstitial hops, the additional interstitial is captured by the I_4 cluster. Figure 2 shows four low-lying core structures of I_5 identified during the PR simulations. With the classical MEAM potential, Fig. 2(a) is the ground state which is found most frequently, independent of the initial configurations. The metastable structures Fig. 2(b)-(d) are characteristic transient structures found at the early stage of the interstitial trap. In all, the I_4 core structure remains intact in I_5 . Further interstitial injection into the cell containing a compact I_5 results in the formation of compact clusters as large as $n=20$.

With *ab initio* calculations, the ground state configuration changes with size: compact for small clusters and, for larger clusters, interstitial chains forming extended $\{311\}$ defects.⁷ Chain-like, elongated clusters are local minimum structures of any interstitial cluster larger than $n=3$. The stability of interstitial chains is achieved by maximizing the ratio of four-fold coordinated atoms to the number of interstitials incorporated into a cluster. The elongated clusters are basic building blocks of extended $\{311\}$ defects.^{7,13} Therefore, the growth mechanism of elongated clusters is an important step in understanding the formation of extended $\{311\}$ defects.

The role of the shape of interstitial traps is investigated by performing PR simulations using chain-like clusters as nuclei for cluster growth. Figure 3 shows the chain structure before and after an interstitial capture. By concerted motions, an interstitial can be easily trapped at the chain end. In the figure, the interstitial chain extends from $n=5$ to 6. This extension releases about 2 eV. We find many trapping paths for various trajectories of an incoming interstitial. Once a metastable elongated clus-

ter is formed, the transition from an elongated shape to a compact one would require bond rearrangements involving many atoms, thus becoming kinetically inaccessible within typical simulation time of 1-10 nsec.

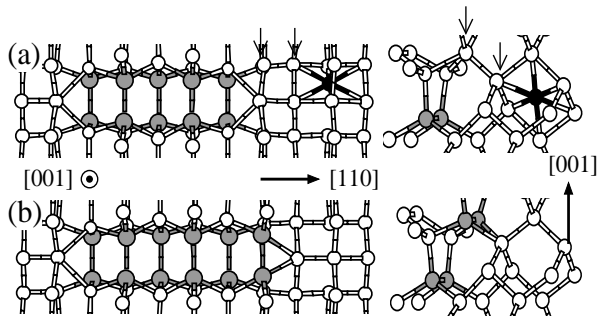


FIG. 3. Schematics for an interstitial trap by an elongated cluster: (a) an interstitial \bullet is placed at the nearest hexagonal site; and (b) an extra chain is formed by concerted motions by an interstitial and the atoms at the end. The gray atoms denote $\langle 110 \rangle$ interstitialcies constituting a chain. The transition from (a) to (b) releases 2 eV.

Although the most energetically favorable trapping occurs at the chain ends, the active capture sites extend the entire interstitial chain. Figure 4 illustrates a growth mechanism for an elongated cluster by an interstitial capture in the middle of a chain, followed by interstitial diffusion steps to the chain end. Seven-member rings surrounding a chain are efficient interstitial trap sites with an interstitial-binding energy of 1 eV. The interstitial captured in the seven-member rings diffuses by making random jumps in the chain direction. Eventually, the interstitial settles at the chain end, releasing an extra 1 eV.

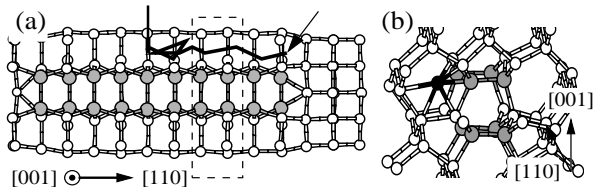


FIG. 4. (a) Schematics for an interstitial trap by an elongated cluster. An interstitial is first trapped in the middle of the chain. The solid line is a trajectory of the interstitial making jumps in the $[110]$ chain direction. Eventually, the interstitial is incorporated into the chain end indicated by the arrow on the right. (b) presents a local minimum configuration, when the interstitial is located in the dotted region.

The interstitial-capture mechanisms of Figs. 3 and 4 lead to the elongation of interstitial chains. Furthermore, they present possible paths for the growth of planar $\{311\}$ defects. When two interstitials captured at seven-member ring sites interact during the random jumps in the chain direction, they form a stable, immobile structure attached to an existing chain. This provides new

trap nuclei for an additional interstitial chain parallel to the existing interstitial chain.

In conclusion, we present parallel-replica simulations using a classical MEAM potential to atomistically model the growth of interstitial clusters. We probe microscopic processes of interstitial-diffusion and interstitial-trapping mechanisms and quantify dynamical properties such as diffusion constants of mobile interstitial defects. As predicted by energetics, interstitial clusters can capture mobile interstitial defects to form more stable, larger clusters. Many local minimum structures for clusters larger than $n=4$ can be accessed by local bonding rearrangements. The shape of interstitial traps plays an important role in determining the shape of final clusters. The elongation of interstitial clusters and the growth of planar $\{311\}$ defects are predicted by the interstitial-capture mechanisms of elongated clusters.

This work is supported by the SRC (contract number: 2000-MJ-759) and the DOE-Basic Energy Sciences, Division of Materials Sciences (contract numbers: Ohio State University DE-FG02-99ER45795; Los Alamos National Laboratory W-7405-ENG-36). Computational resources are provided by OSC, NCSA, and NERSC.

-
- ¹ D. J. Eaglesham, P. A. Stolk, H.-J. Gossmann, and J. M. Poate, *Appl. Phys. Lett.* **65**, 2305 (1994).
 - ² L. H. Zhang, K. S. Jones, P. H. Chi, and D. S. Simons, *Appl. Phys. Lett.* **67**, 2025 (1995).
 - ³ N. E. B. Cowern *et al.*, *Phys. Rev. Lett.* **82**, 4460 (1999).
 - ⁴ M. Jaraiz, G. H. Gilmer, J. M. Poate and T. D. de la Rubia, *Appl. Phys. Lett.* **68**, 409 (1996).
 - ⁵ N. Arai, S. Takeda, and M. Kohyama, *Phys. Rev. Lett.*, **78**, 4265 (1997).
 - ⁶ J. Kim, F. Kirchhoff, W. G. Aulbur, J. W. Wilkins, and F. S. Khan, *Phys. Rev. Lett.* **83**, 1990 (1999).
 - ⁷ J. Kim, F. Kirchhoff, J. W. Wilkins, and F. S. Khan, *Phys. Rev. Lett.* **84**, 503 (2000).
 - ⁸ B. J. Coomer, J. P. Goss, R. Jones, S. Öberg, and P. R. Briddon, *J. Phys. Condens. Matter* **13**, L1 (2001).
 - ⁹ A. Bongiorno, L. Colombo, F. Cargnoni, C. Gatti and M. Rosati, *Euro. Phys. Lett.* **50**, 608 (2000).
 - ¹⁰ A. F. Voter, *Phys. Rev. B* **57**, R13985 (1998).
 - ¹¹ T. J. Lenosky, B. Sadigh, E. Alonso, V.V. Bulatov, T. Diaz de la Rubia, J. Kim, A.F. Voter and J.D. Kress, *Model. Simul. Mater. Sci. Eng.* **8**, 825 (2000).
 - ¹² M. I. Baskes, *Phys. Rev. B* **46** 2727 (1992).
 - ¹³ S. Takeda, *Jpn. J. Appl. Phys.* **30**, L639 (1991); M. Kohyama and S. Takeda, *Phys. Rev. B* **46**, 12305 (1992).